frontiers | Frontiers in Marine Science

ORIGINAL RESEARCH
published: 01 June 2022
doi: 10.3389/fmars.2022.921726

Identification and Functional Analysis of the G1 Phase Cyclin Dependent Kinase Gene *Hc-CDK6* in Pearl Mussels (*Hyriopsis cumingii*)

ShangLe Feng[1†], *XueNan Li*[1†], *He Wang*[1], *WenJuan Li*[1,2,3*] *and ZhiYi Bai*[1,2,3*]

[1] Key Laboratory of Freshwater Aquatic Genetic Resources, Ministry of Agriculture, Shanghai Ocean University, Shanghai, China, [2] Shanghai Engineering Research Center of Aquaculture, Shanghai Ocean University, Shanghai, China, [3] Shanghai Collaborative Innovation Center for Cultivating Elite Breeds and Green-culture of Aquaculture Animals, Shanghai, China

OPEN ACCESS

Edited by:
Xiaotong Wang,
Ludong University, China

Reviewed by:
Gen Hua Yue,
Temasek Life Sciences Laboratory, Singapore
Zhongming Huo,
Dalian Ocean University, China

***Correspondence:**
ZhiYi Bai
zybai@shou.edu.cn
WenJuan Li
wjli@shou.edu.cn

[†]These authors have contributed equally to this work

Specialty section:
This article was submitted to Aquatic Physiology, a section of the journal Frontiers in Marine Science

Received: 16 April 2022
Accepted: 06 May 2022
Published: 01 June 2022

Citation:
Feng S, Li X, Wang H, Li W and Bai Z (2022) Identification and Functional Analysis of the G1 Phase Cyclin Dependent Kinase Gene Hc-CDK6 in Pearl Mussels (Hyriopsis cumingii). Front. Mar. Sci. 9:921726. doi: 10.3389/fmars.2022.921726

Cyclin dependent kinase 6 (CDK6) is a serine/threonine kinase that plays important roles in cell cycle progression and differentiation. In this study, full-length cDNA of *Hc-CDK6* was obtained from freshwater pearl mussels (*Hyriopsis cumingii*, *Hc*) with 3′,5′ rapid-amplification of cDNA ends (RACE). The *Hc-CDK6* expression profiles were analyzed with quantitative real-time PCR and *in situ* hybridization. The function of the *Hc-CDK6* gene was studied with both RNA interference (RNAi) and overexpression in *H. cumingii*. *Hc-CDK6* was found to encode 331 amino acids and to have a CDK4/6-like serine/threonine kinase catalytic structural domain. In terms of the amino acid sequence, the protein Hc-CDK6 was most closely related to its homolog in *Crassostrea gigas*, with a similarity of 75.23%. *Hc-CDK6* was expressed in all examined tissues (adductor, foot, visceral mass, gill, outer mantle, inner mantle and gonads), and the highest expression was observed in the gonads ($P<0.05$). The relative expression of *Hc-CDK6* increased during embryonic development, and was higher in the blastocyst and gastrulation stages, which were characterized by rapid division and differentiation. *Hc-CDK6* showed hybridization signals in all parts of the mantle. After knockdown of *Hc-CDK6* through RNAi, a significant decrease in *CDK6* expression was found, and the percentage of cells in G0/G1 significantly increased. Overexpression of *Hc-CDK6* in mantle cells increased the proliferation of cultured cells ($P<0.05$). *Hc-CDK6* appeared to promote the cell cycle in *H. cumingii*, and overexpression of *Hc-CDK6* promoted mantle cell proliferation. The functional study of this gene may provide new ideas for solving the problem of slow proliferation of shellfish cells in *in vitro* culture.

Keywords: ***Hyriopsis cumingii*, Hc-CDK6, cell cycle, RNAi, overexpression**

1 INTRODUCTION

Cell division is the most fundamental developmental process in unicellular or multicellular organisms, and the cell cycle describes the entire process of cell division from the end of the last mitosis to the completion of the next mitosis (Jacobs, 1992). This process is tightly regulated by cyclins and cyclin dependent kinases (CDKs) (Satyanarayana and Kaldis, 2009; Lim and Kaldis,

2013). CDKs play important roles in cell cycle checkpoints in eukaryotic cells, and cells entering S-phase must meet the basic requirements for CDK activation (Massague, 2004).

Each CDK has a structural domain consisting of a cyclin-binding domain and a T-loop motif that together participate in CDK activation. During the cell cycle, CDK protein amounts are essentially unchanged, and these kinases interact with different cyclins and form active complexes (Pines and Hunter, 1991; Malumbres et al., 2009; Suryadinata et al., 2010). CDKs are catalytic subunits that are activated by the corresponding cyclins. The CDK6-Cyclin D complex regulates cell proliferation through the G1-S checkpoint (Pietenpol and Stewart, 2002). This complex has kinase-dependent and independent functions and is a hub for the integration of signals affecting transcription, proliferation and differentiation (Tigan et al., 2016). Current research on CDK6 focuses on tumor and cancer-related aspects. Overexpression of CDK6 is often used as a biomarker for tumor diagnosis, and its overactivation leads to uncontrolled cell proliferation (Baba et al., 2014). Given the role of CDK6 in cell cycle regulation, many studies have achieved antitumor effects by inhibiting the activity of CDK6 (Schaer et al., 2018). In aquatic organisms, CDK6 has been less studied, and only cloning and tissue expression analysis of CDK6 in *Scophthalmus maximus* have been performed; however, further study of its function is lacking (Guo et al., 2016). The function of CDK6 in aquatic organisms remains poorly understood.

H. cumingii is an important freshwater pearl mussel: 95% of the freshwater pearls worldwide are produced by *H. cumingii*, which has high economic and research value (Wang et al., 2021a). In production, defective pearls such as tail pearls and specially shaped pearls may be formed through the influence of nuclear insertion technology, pearl breeding and other factors (Pan and Wen, 2002). The mantle is an important site not only for pearl formation but also for making mantle saibos. Some researchers have studied the cultivation of pearls with free mantle cells instead of mantle saibos, and have found that the number of defective pearls produced by mantle free cells significantly decreases, but the activity and proliferation of cells affect the formation of pearls (Qian et al., 2002; Jin et al., 2011; Li et al., 2014). In cell cycle regulation, late G1 and G2/M limited points phases determine whether a cell is in a proliferative or quiescent state (Fu et al., 1999; Pietenpol and Stewart, 2002). It is reported that with the increase in mantle cells with culture time, the number of G0/G1 phase cells increases significantly, thus indicating that, over the course of culture, some cells might not be able to pass the late G1 limited point, and the cell proliferation activity decreases (Cao et al., 2020). The important regulatory role of CDK6 in the G1 phase of the cell cycle is crucial for enhancing the proliferation of mantle cells *in vitro*.

In this study, we identified *Hc-CDK6* in *H. cumingii*, and analyzed their expression in different tissues and developmental stages of embryo. The effect of *Hc-CDK6* silencing and overexpression on the expression of *Hc-CCND2* and distribution of the cell cycle were investigated. These results will be helpful to understand the regulation of the shellfish cell cycle. and provide a novel approach for improving the slow proliferation rate of shellfish cells in *in vitro* cultures.

2 MATERIALS AND METHODS

2.1 Animals and Tissue Samples

Healthy 1-year-old mussels (*H. cumingii*, 15 individuals, 6–7 cm shell length) were collected from a farm in Wuyi (Zhejiang, China) in March, 2021.

Cut off the adductor from selected mussels, the tissues were sampled respectively. The samples used in the experiment included the adductor, foot, gill, outer mantle, inner mantle and gonads. Embryo samples were sampled from adult mussels' gill tissue at 1 day, 3 day, 5 day, 7 day, 9 day, 10 day, including the cleavage stage, blastula stage, gastrula stage, and glochidium. All samples were immediately frozen in liquid nitrogen and stored at - 80°C (Wang et al., 2021b).

For suspension cell preparation, the adductors were cut off from selected mussels with a scalpel, and the mantle and gill tissues were repeatedly washed with sterile distilled water. The outer mantle was then separated and cut into small pieces (1 mm^2). After digestion in 0.25% trypsin at 37°C for 20 min, excess tissue mass was filtered through a 300 mesh strainer. The cell suspension was counted with a hemocytometer, the cell number was adjusted to 5×10^5 to 1×10^6 mL^{-1} used 1640 medium, and cultured in a constant temperature incubator at 25°C. The medium formula is 500 μL sodium pyruvate, 500 μL nonessential amino acid, 5 mL fetal bovine serum and 44 mL of 1640 basal medium.

2.2 Amplification of Full-Length cDNA

Total RNA was extracted with RNAiso Plus (TaKaRa, Japan). The RNA concentration and quality were detected with a spectrophotometer (Thermo Fisher Scientific, USA) and 1% agarose gel, respectively. Partial cDNA sequences of *Hc-CDK6* were obtained from the transcriptome of *H. cumingii* (unpublished). Primers were designed with NCBI Primer BLAST (https://www.ncbi.nlm.nih.gov/tools/primer-blast/) for sequence verification. After reverse transcription of RNA (TransGen Biotech, China), the obtained cDNA was used for sequence verification.

The 3' and 5' ends of *Hc-CDK6* cDNA were amplified through the RACE method with a SMARTer® RACE 5′/3′ Kit (Takara Bio, USA). The primers were designed on the basis of partial *Hc-CDK6* sequences verified with an NCBI primer Blast search (**Table 1**). The PCR product was purified with a Gel Extraction Kit (TaKaRa, Japan) according to the manufacturer's instructions, then incubated with pMD19-T (TaKaRa, Japan) at 16°C for 4 h. Subsequently, ten μL of the above incubation products was transformed into DH5α cells. PCR positive clones were selected and subjected to sequencing with 3730xlDNAAnalyzer by GENEWIZ, Inc (Suzhou). The 3' and 5' sequences were spliced to obtain the full length cDNA.

2.3 Sequence and Phylogenetic Analysis

Prediction of Hc-CDK6 amino acid sequences was performed with the NCBI ORF finder online tool (https://www.ncbi.nlm.nih.gov/orffinder/). Prediction of Hc-CDK6 amino acid signal peptides was performed with SignalP4.1 (http://www.cbs.dtu.dk/services/SignalP/). Hc-CDK6 phosphorylation sites were

TABLE 1 | Primers used in isolation and characterization of *Hc-CDK6* in pearl mussels.

Primer name	Purpose	Sequence (5′ to 3′)
CDK6-F	Sequence	CAGAACACGGAGGAAGGCAT
CDK6-R	verification	TGGCAGGGAGACATTTTCCG
5' outer	5′ RACE	TGGCCAATCTACTTCCGGTGGTCT
5' inner		TCCACTGGGGTGGCATACTGGGC
3' outer	3′ RACE	GGGCTGGGCCCTGACAAAATCAG
3' inner		ACAGGCCCAGTATGCCACCCCA
qRT-PCR-F	*CCND2*	GATAGCAGCAGGGAGTGT
qRT-PCR-R	qRT-PCR	TTTGTGGATTCCGTTTCG
EF1α-F	reference gene	GGAACTTCCCAGGCAGACTGTGC
EF1α-R		TCAAAACGGGCCGCAGAGAAT
T7-G1-F	DsRNA	GGATCCTAATACGACTCACTATAGG
T7-G1-R		TGCAGCTCCTAAATGGGGTG
G1-F		GGATCCTAATACGACTCACTATAGG
G1-R		GCACTAATTCGTTGGTGGGG
		TGCAGCTCCTAAATGGGGTG
		GCACTAATTCGTTGGTGGGG
T7-G2-F	DsRNA	GGATCCTAATACGACTCACTATAGG
T7-G2-R		CCGACTTTGCCACGATTCAG
G2-F		GGATCCTAATACGACTCACTATAGG
G2-R		ACCACAAGGTGACCACAACT
		CCGACTTTGCCACGATTCAG
		ACCACAAGGTGACCACAACT
T7-G3-F	DsRNA	GGATCCTAATACGACTCACTATAGG
T7-G3-R		CTAGCGGATTTTGGTCTCGC
G3-F		GGATCCTAATACGACTCACTATAGG
G3-R		AGACGAGGGACTAGAGGTT
		CTAGCGGATTTTGGTCTCGC
		AGACGAGGGACTAGAGGTT
q-CDK6-F	*CDK6* qRT-PCR	AGTTGTGGTCACCTTGTGGT
q-CDK6-R		TGGCCAATCTACTTCCGGTG
P- CDK6-F	Plasmid	TCGAGCTCAAGCTTCGAATTCATGA
P- CDK6-R	construction	GCCGACTTTGCCACG GTACCGTC
CDK6-ISH-F	Probe synthesis	GACTGCAGAATTCTCA
CDK6-ISH-R		TTTGCTGACAGGTGTATCCG
		AGTTGTGGTCACCTTGTGGT
		GGATCCTAATACGACTCACTATAGG
		TGGCCAATCTACTTCCGGTG

analyzed using NetPhos 3.1 (http://www.cbs.dtu.dk/services/NetPhos/), and isoelectric points and molecular weights were predicted with the Compute pI/Mw tool (https://web.expasy.org/compute_pi/). Multiple comparisons of amino acid sequences and phylogenetic tree construction (neighbor-joining method, 1000 bootstrap replicates) were performed in Bioedit and MEGA7.0, respectively.

2.4 Expression Analysis of *Hc-CDK6* by qRT-PCR

The RNA extraction method for frozen samples was as described in section 2.2. The manufacturer's instructions for PrimeScript™ RT Master Mix (TaKaRa, Japan) were followed for reverse transcription of RNA samples. The information on quantitative primers and reference primers used to examine tissues and embryo expression levels is shown in **Table 1**. *Hc-CDK6* relative expression were detected with the CFX96 system (Bio-Rad, USA), each sample was performed on three technical replicates. The qRT-PCR reaction conditions followed the TB Green® Fast qPCR Mix instructions (TaKaRa, Japan). Relative expression of *Hc-CDK6* was calculated with the $2^{-\Delta\Delta CT}$ method.

2.5 In Situ Hybridization

The cDNA fragments were synthesized with probe synthetic primers (**Table 1**), then purified and subjected to *in vitro* transcription (Transgen, China). The probes were labeled with DIG RNA Labeling Mix. Healthy *H. cumingii* (1 year old) were selected, and the mantle tissue (5×8 mm) was cut and fixed in 4% paraformaldehyde for 18 h. The tissue was then dehydrated in alcohol, rendered transparent in xylene and finally embedded in paraffin. A paraffin slicer was used to slice sections with a thickness of 3 μm. The *in situ* hybridization procedure was performed according to the *in situ* hybridization kit instructions (Boster, USA). Samples were observed and photographed under a microscope.

2.6 Synthesis of dsRNA *In Vitro*

According to the sequence of the ORF region of *Hc-CDK6*, three pairs of primers approximately 500 bp in length were designed with NCBI Primer BLAST. We added a T7 sequence to the 5' end of each primer pair. The primers were amplified and purified to obtain the target sequence. The *in vitro* transcription of target sequences was performed according to the instruction manual (TransGen Biotech, China). The dsRNA was obtained as previously described (Wang et al., 2021). After purification, dsRNAs were diluted to working concentration (300 ng/μL) with RNase/DNase-free water.

2.7 Knockdown of the *CCND2* Gene *In Vivo* by RNAi

Sixty healthy 1-year-old *H. cumingii* (average weight 55 ± 2 g) were randomly assigned to four groups (15 individuals/group). Three groups were randomly selected as experimental groups to be injected with 100 μL of the corresponding dsRNA. The negative control group was injected with 100 μL of RNase/DNase-free per mussel. Gill tissue was collected from each group at three time points post-injection (n=5, at 24 h, 48 h and 72 h). The tissue collection and preservation methods were as described in section 2.1, and the RNA extraction and reverse transcription methods were as described in sections 2.2 and 2.4, respectively.

After RNAi, we used flow cytometry to analyze cell cycle phases. Briefly, gill cells were collected from mussels after RNAi. The gill tissue suspension cell collection method was as described in section 2.1. Cells were collected after removal of culture medium, and washed and fixed according to the manufacturer's instructions for PI/RNase Staining Buffer (BD, USA). The cells were then resuspended in 500 μL PI/RNase solution (BD, USA) for 15–20 min in the dark in a 37°C incubator. Samples were analyzed with an Accuri C6 Plus Cytometer (BD Biosciences, USA). The numbers of cells in the different cell cycle phases were calculated.

2.8 Overexpression of *Hc-CDK6* Gene in Mantle Cells

The ORF region of the *Hc-CDK6* gene was amplified by PCR, and the purified PCR product was used in plasmid construction (**Table 1**). The restriction enzyme site was *EcoR* I (GAATTC). The pcDNA3.1 vector (Clontech, USA) was digested with *EcoR* I.

The purified PCR product was ligated into the pcDNA3.1 vector with a Seamless Cloning Kit (Beyotime Biotechnology, China), and the plasmids were transformed into DH5α cells. Finally, single clones were selected for sequence identification (GENEWIZ, China).

In the transient transfection experiments, pcDNA3.1-CDK6 plasmids (2.5 μg) were transfected with Lipo8000 (Beyotime, China) according to the user manual. Cell growth state was observed under an inverted microscope (Olympus, Japan) during cell culture, and pictures were taken. Cell proliferation was assessed in normal mantle cells and *Hc-CDK6* overexpressing mantle cells with CCK-8 dye (Beyotime, China). Analysis of the cell cycle after transfection was performed by flow cytometry.

2.9 Statistical Analysis

All data were analyzed with one-way analysis of variance. Data are expressed as mean ± SE. Multiple comparisons between groups were analyzed with Duncan's multiple range tests. A value of $P<0.05$ was considered significant. OriginPro 9.1 (OriginLab, Massachusetts, USA) was used to plot bar charts.

3 RESULTS

3.1 Obtained and Characterization of *Hc-CDK6* cDNA Clones

The complete cDNA sequence of *Hc-CDK6* was obtained with RACE, was deposited in GenBank accession number **OM572509**. The full length cDNA was 1,818 bp, the ORF was 996 bp, and the 5'UTR and 3'UTR were 228 bp and 594 bp, respectively (**Figure 1**). A typical polyadenylation signal sequence was found in the 3'UTR. The ORF of the *Hc-CDK6* cDNA encoded 331 aa.

Amino acid analysis indicated that Aa 13–300 contained the catalytic structural domain of a CDK4/6-like serine/threonine kinase, and amino acid residues bound to D-type cyclins are

```
1     cacggagcgc tgtaatcgag ctcggtcccg gggatcctct agagatctaa tacgactcac
61    tatagggcaa gcagtggtat caacgcagag tacatgggga gatttctgtg taccaccagt
121   ggcagcctac acgcgtaaac taggaatcaa cttgtttggg aagtaacgta atgttgtgtg
181   aagaaaaatt cagaaaaaat cgtggaaata ttgaattcgt tcaaatatgg gttgatcatt
241   tttgtagaaa ctcgatgcac atattgaaca gcgcaaatct tacacacttt tggaaacact
301   tgtgatgtca tttcaatgca catatcatga gccgactttg ccacgattca ggagaaaatg
361   catatgagga ggtagcagtg attggaaatg gagcatatgg aactgtgtgg aaggccagag
421   accttaagaa tgatggccag tttgtggcca tgaaaaaaat cagaattcag aacacggagg
481   aaggcatgcc tatgagtgca attcgagaaa ttgcactact tcggcaactt gaaggtcatg
541   aacatcccaa tattgtgagg ctgctggatg taagaacaca cagccaagaa aaatctgaaa
601   tcagccttat tttggtgttt gaatacatcg accaagattt atccacatac ttggaaaggt
661   gccctaaccc agggctgggc cctgacaaaa tcagggacct tatgttgcag ctcctaaatg
721   gggtggattt tctgcactca aaccgaattg tccatcgtga tctcaagcca caaaatattc
781   ttgtcacaag tcaaggtaga ctgaagctag cggattttgg tctcgccaga gtttatggct
841   ttcagatggc gttaacacaa gttgtggtca ccttgtggta tagagcccct gaggtcatcc
901   tacaggccca gtatgccacc ccagtggata tgtggagctg tgggtgtata tttgctgaac
961   tctacaacag aagaccactt ttctgtggac agtctgatat tgaccagcta ataaagatat
1021  ttgaaatgct tggaagacca ccggaagtag attggccaga aaatgtctcc ttgccatgga
1081  gttcgtttaa agcatatcca tcacagcaac ttacaaaata cattccagag atagatccaa
1141  tagccaagga cttgctagag aagttattga aattcaatcc ccaccaacga attagtgcca
1201  aaaatgcatt gaatcaccaa tactttcgtg atgaaataga tgacatacga acctctagtc
1261  cctcgtctgt tttggagagt aattctagtg atggaagatc ggatacacct gtcagcaaat
1321  gaacagaatc tcagtgtgat cgggaataat tgtgataaag aagaatcatg ggaactgagt
1381  caagttccag atgttgaaag caattacagt tgtaatcttg tctgctgttc tgccattttc
1441  acaaaacttt ctcatgcctg agatattccg atgtgatttc caggaatggc gaaatttgtt
1501  gatttgagga atataactga caaccctgtt gaccagtgac ataaagttta tacagtaggg
1561  tgaacatatt gtatacactt gcttttgtgt ccagctgcaa actgcacaga ccgagatctg
1621  ccctcacata atgcactagc agatctgggt ctgtgcagtt tgttaggagt aatcagtaga
1681  acaagacaga acctaatccg caggtgcatt atgatacaac agatcatggg ttattggaat
1741  ttgacatgac ttaaaagcgt atatatatgt atgtatgtat gtatgtatgt atgtatgtac
1801  gtacgtacgt acgtacgtac gtatgtatgt atatatatat atggtgagtg tttgtaaggt
1861  tgagatggtt ttgaaaggtt tgaataataa ggaaaaaaaa aaaaaaaaaa aaaaaa

1     MSRLCHDSGENAYEEVAVIGNGAYGTVWKARDLKNDGQFVAMKKIRIQNTEEGMPMSAIR
61    EIALLRQLEGHEHPNIVRLLDVRTHSQEKSEISLILVFEYIDQDLSTYLERCPNPGLGPD
121   KIRDLMLQLLNGVDFLHSNRIVHRDLKPQNILVTSQGRLKLADFGLARVYGFQMALTQVV
181   VTLWYRAPEVILQAQYATPVDMWSCGCIFAELYNRRPLFCGQSDIDQLIKIFEMLGRPPE
241   VDWPENVSLPWSSFKAYPSQQLTKYIPEIDPIAKDLLEKLLKFNPHQRISAKNALNHQYF
301   RDEIDDIRTSSPSSVLESNSSDGRSDTPVSK
```

FIGURE 1 | The nucleotide and amino acid sequences of *Hc-CDK6* cDNA.

present in this structural domain (**Figure 2**). Predictions indicated the absence of signal peptide sequences and transmembrane structures in this protein. The secondary structure of the protein comprised 30.21% α-helix, 17.22% extended strand and 52.57% random coil. The predicted molecular weight and theoretical isoelectric point were 37773.18 Da and 5.81, respectively.

Amino acid comparison indicated 75% sequence identity with *Mizuhopecten yessoensis* CDK6, 75.23% with *Crassostrea gigas* CDK6 and 74.61% with *Crassostrea virginica* CDK6 (**Figure 2**). The phylogenetic tree was constructed with MEGA7.0 (**Figure 3**), and the Hc-CDK6 amino acid sequence was compared with other available CDK6 sequences. The phylogenetic tree showed that Hc-CDK6 clustered with other marine bivalve sequences.

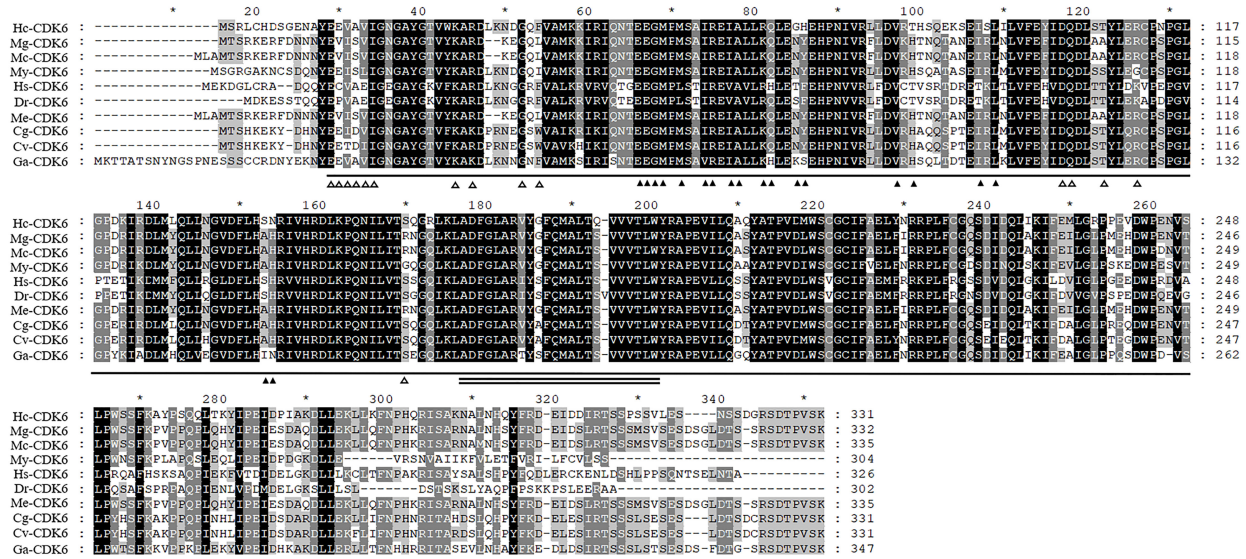

FIGURE 2 | Alignment analysis of Hc-CDK6 with homologous sequences in other species. ▲Indicates the amino acid residue of CDK binding to CCND, △indicates the amino acid residue of CDK binding to INK4, a horizontal line indicates the catalytic domain of cyclin-dependent kinase 4 and 6-like serine/threonine kinases of CDK6, and the double solid line indicates the activation loop (A-loop). GenBank accession numbers: *Mytilus galloprovincialis* (Mg), VDI04144.1; *Mytilus coruscus* (Mc), CAC5413630.1; *Mizuhopecten yessoensis* (My), XP_021356142.1; *Homo sapiens* (Hs), NP_001138778.1; *Danio rerio* (Dr), NP_001137525.1; *Crassostrea gigas* (Cg), XP_011426627.1; *Crassostrea virginica* (Cv), XP_022322423.1; *Gigantopelta aegis* (Ga), XP_041371365.1; *Mytilus edulis* (Me), CAG2221073.1. Black, conserved amino acid residue; gray, analogous residues. * Indicates that starting from the 10th amino acid, every 20 amino acids are marked with a *.

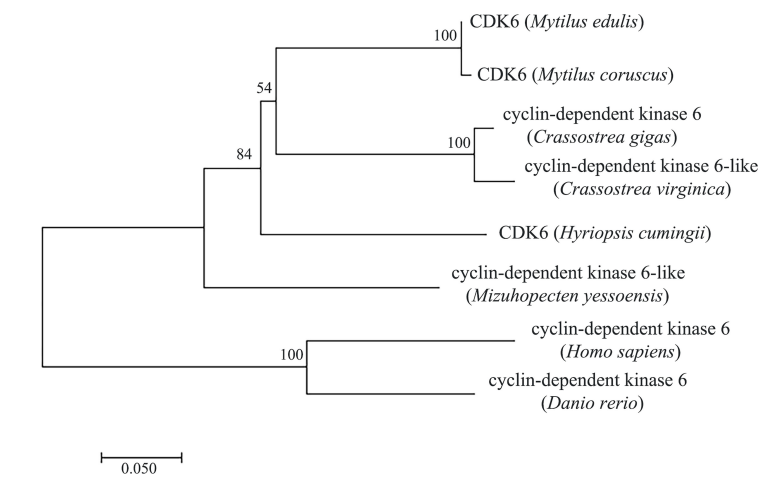

FIGURE 3 | NJ tree of the Hc-CDK6 amino acid sequence with CDK6 sequences from other species. GenBank accession numbers are as in **Figure 2**, the number on the node indicates the confidence value of the test for 1000 Bootstrap repetitions.

3.2 Expression Profiles of *Hc-CDK6* in Different Tissues and Embryonic Periods

The expression level of the *Hc-CDK6* gene in *H. cumingii* tissues was detected with qRT-PCR (**Figure 4A**). *Hc-CDK6* was distributed in the gonads, gills, adductor, foot, outer mantle and inner mantle. The expression of *Hc-CDK6* was highest in the gonads, then in the foot and gills, and was lowest in the adductor; the level in the outer mantle was higher than that in the inner mantle ($P<0.05$).

The qRT-PCR showed that *Hc-CDK6* was expressed in different embryonic stages. The expression of *Hc-CDK6* first increased and then decreased with embryonic development, and the relative expression was highest in the gastrula stage, then decreased in the glochidium stage (**Figure 4B**).

3.3 Localization of *Hc-CDK6* in the Mantle

In situ hybridization was performed to explore the localization of *Hc-CDK6* in the mantle tissue. **Figures 5A, B** shows the *in situ* hybridization of the experimental and control groups, respectively. Compared with the control, *CDK6* showed positive hybridization signals in all parts of the mantle, on the outer fold as well as on the middle fold (at the arrow), and *CCND2* showed positive hybridization signals on the ventral mantle, the outer fold as well as the middle fold (**Figure 5C**, at the arrow), whereas no hybridization signals were present in the control.

3.4 Knockdown of *Hc-CDK6* Induces Cell Cycle Arrest in Gill Cells

The three interfering chains were synthesized for screening, and the qRT-PCR results of the mantle and gill tissues after the injection of the three interfering chains showed that the expression of the three interfering chains was significantly lower in the gill tissues than that in the control group after RNAi ($P<0.05$). The highest knockdown rates were 76.3%, 88.4% and 51.7% in the gills on the 2nd day (**Figure 6A**). In the mantle tissues, the expression of *Hc-CDK6* significantly differed from that in the control group on the 2nd day ($P<0.05$), but the knockdown efficiency was lower than that in gill tissues (**Figure 6B**). Interfering chain 2, which had the highest knockdown rate, was selected for RNAi, and gill tissue was selected for downstream gene expression detection and flow cytometric analysis.

After RNAi, the relative expression of *Hc-CCND2* (**Figure 6D**) and *Hc-CDK6* (**Figure 6C**) was significantly lower than that in the control groups ($P<0.05$). Pearson analysis showed a significant positive correlation between *Hc-CCND2* and *Hc-CDK6* relative expression after knockdown ($P<0.05$).

The percentage of G0/G1 phase cells increased significantly, and the percentage of S phase cells decreased significantly after *Hc-CDK6* RNAi ($P<0.05$, **Figure 7**). The cell proliferation index was calculated and analyzed, and also showed a significant decrease after RNAi ($P<0.05$).

3.5 Overexpression of *Hc-CDK6* Promotes Mantle Cell Proliferation

After transfection, no significant difference was observed in cell number compared with that in the control group ($P>0.05$, **Figure 8**), after analysis with a hemocytometer. Cell proliferation viability assays showed that the cell proliferation viability was significantly higher ($P<0.05$) than that in the control group at the fourth day of culture after transfection (**Figure 9**).

The cell cycle percentage after plasmid transfection was analyzed with flow cytometry. After pcDNA3.1-CDK6 plasmid transfection, the percentage of G1 phase cells in the recombinant plasmid group was significantly lower than that in the blank and empty plasmid groups ($P<0.05$), and the calculated PrI was significantly higher in the recombinant plasmid group than the control groups ($P<0.05$, **Table 2**).

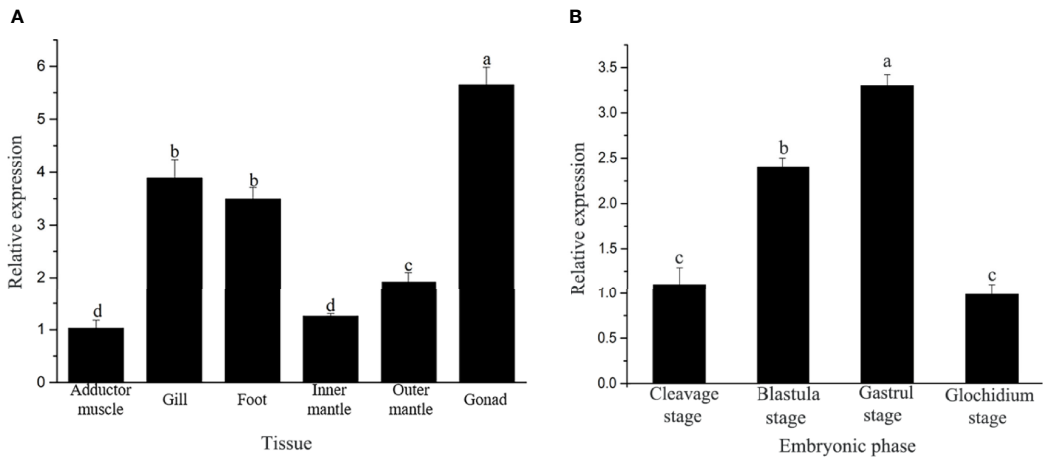

FIGURE 4 | **(A)** Analysis of relative *Hc-CDK6* expression levels in different tissues. **(B)** *Hc-CDK6* expression levels during different embryonic periods. Values with different letters indicate $P < 0.05$.

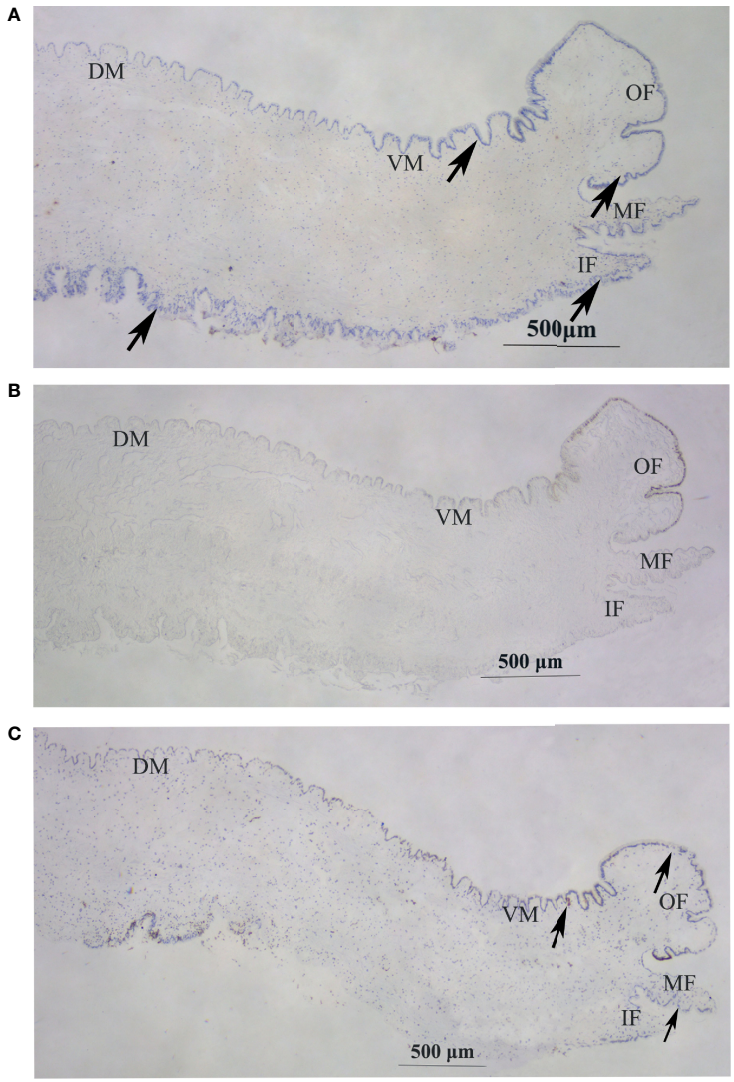

FIGURE 5 | *In situ* hybridization in the mantle of *H. cumingii*. **(A)** Signal of *Hc-CDK6* in the experimental groups. **(B)** Micrograph of the control groups. **(C)** Signal of *Hc-CCND2* in experimental groups. The arrow indicates the position of the signal. OF, outer fold; MF, middle fold; IF, inner fold; DM, dorsal mantle; VM, ventral mantle.

4 DISCUSSION

CDK4/6 and CDK2 are the first kinases activated by mitogenic signals that release cells from the G0 block (Park and Krause, 1999), which regulate cell cycle progression (Kozar and Sicinski, 2005). The amino acid residues that bind D-type cyclins and INK4 were also found in the amino acid sequence of Hc-CDK6, thus indicating that this kinase is a typical CDK family protein, in agreement with findings reported by Guo Jiawei et al. (Guo et al., 2016). Amino acid similarity comparison indicated that this domain was highly similar to those in other species. Thus, Hc-CDK6 might function similarly to homologs in other species and co-regulate the G1-S phase transition with D-type cyclins and CKIs. Phylogenetic tree analysis indicated that the *H. cumingii* CDK6 sequence clustered with those of marine bivalves such as oysters and scallops, and was furthest from those of vertebrates, thus indicating that Hc-CDK6 is highly evolutionarily conserved.

CDK6 plays an important role in cell cycle progression and differentiation (Ericson et al., 2003; Musgrove et al., 2011). The expression of CDK6 was highest in tissues with fast growth and development, such as the gonads in *Scophthalmus maximus* (Guo et al., 2016). This finding is consistent with the expression characteristics of *H. cumingii CDK6* in this study. The similarity in tissue expression between *Hc-CDK6* and *Hc-CCND2* (on the basis of previous experiments) also suggested their synergistic role in the cell cycle process. The cleavage and blastocyst stages involve rapid division of embryonic cells, and gastrulation is a process of regular migration, arrangement

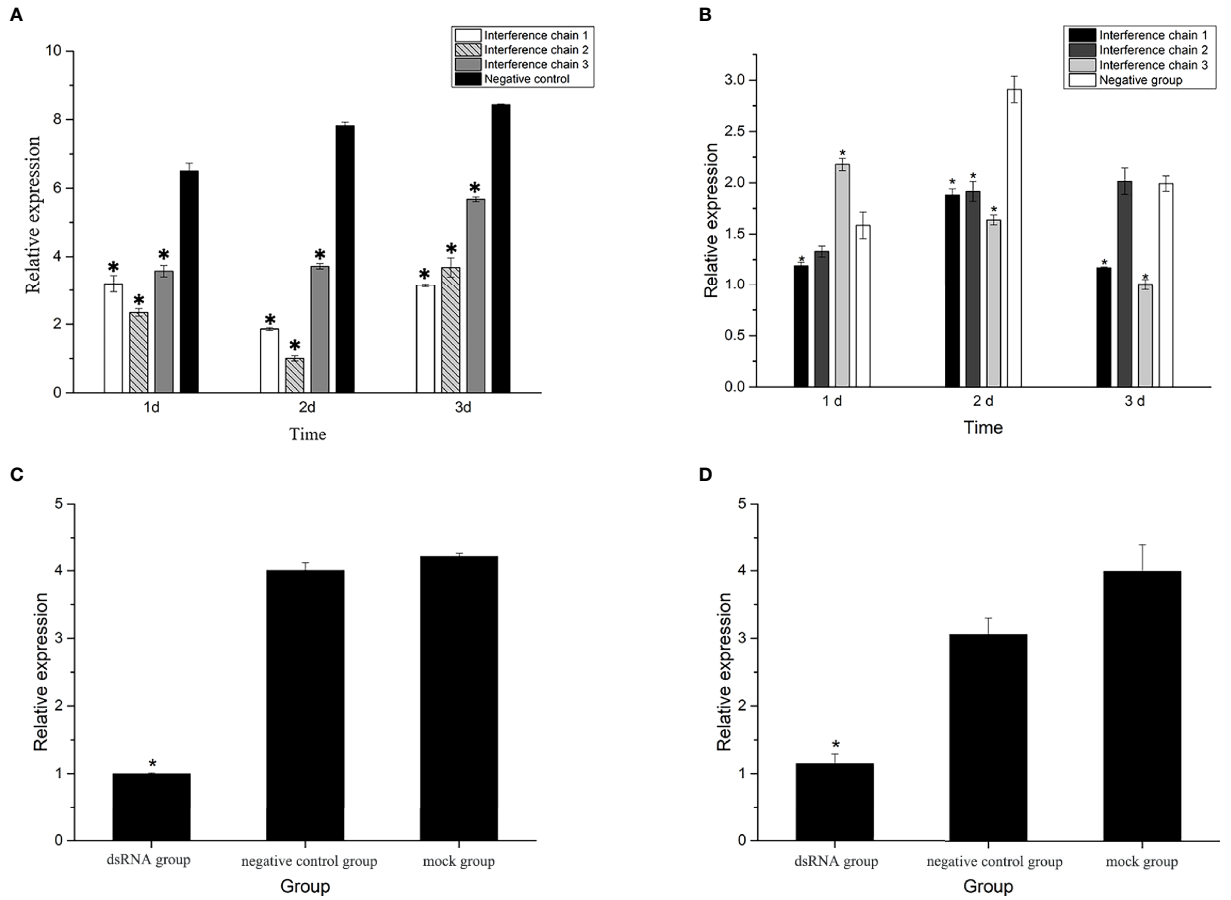

FIGURE 6 | **(A)** Relative expression of *Hc-CDK6* in the gills after RNAi at three time points. **(B)** Relative expression of *Hc-CDK6* in the mantle after RNAi at three time points. **(C)** Relative expression of *Hc-CDK6* in group 2, and the negative control and blank groups. **(D)** Relative expression of *Hc-CCND2* in group 2, and the negative control and blank groups. *Significance level ($P < 0.05$).

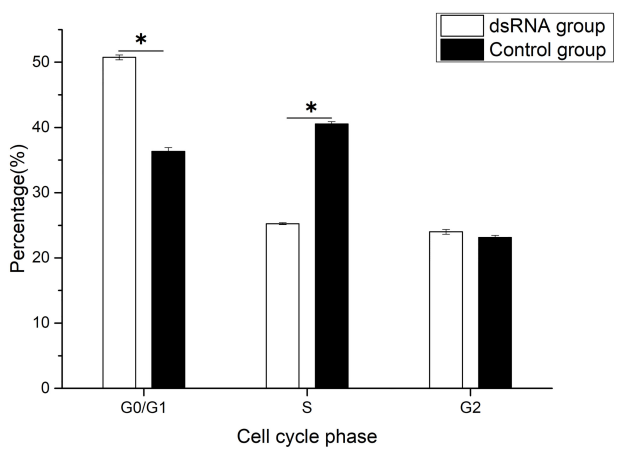

FIGURE 7 | Cell cycle phase distribution of gill cells in *Hyriopsis cumingii* after *Hc-CDK6* RNAi, *Significant difference ($P < 0.05$), Maximum value of vertical axis is 100%.

and differentiation of embryonic cells (Eyal-Giladi and Kochav, 1976; Lin et al., 2010). The increase in CDK6 expression during embryonic development also indicates that this protein is closely associated with the rapid division and differentiation of early embryonic cells, in agreement with the results of Guo Jiawei et al. (Guo et al., 2016).

In situ hybridization of the mantle showed different hybridization signal sites of *Hc-CDK6* and *Hc-CCND2*. CCND2 is closely associated with cell proliferation, and quantitative and *in situ* hybridization results indicated that the outer mantle is more viable than the inner mantle. CDK is the core regulatory molecule of the cell cycle. CDK expression tends to be stable during the cell cycle, and it is activated by the corresponding cyclins, which are expressed periodically, and then participate in cell cycle regulation (Jacobs, 1992; Malumbres and Barbacid, 2009; Lim and Kaldis, 2013). In this study, the extensive hybridization signals of CDK6 showed that mantle cells had proliferation potential, and its different localization and expression characteristics from those of CCND2 also indicated that cells in different locations in the

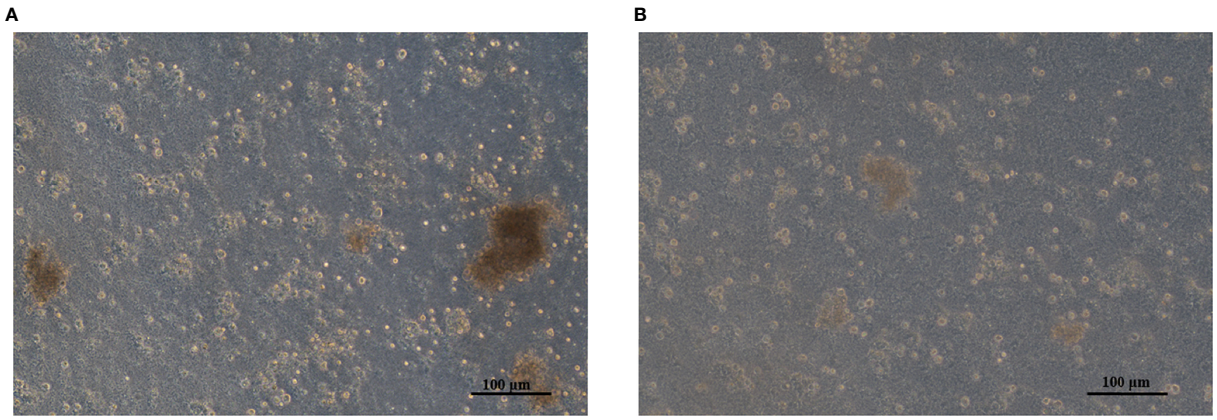

FIGURE 8 | **(A)** Adherent mantle cells in the pcDNA3.1-CDK6 transfection group. **(B)** Mantle cells in the control group.

mantle may vary in their proliferation states. CCND2 and CDK6 are closely related in the cell cycle, and their different localization and expression characteristics must be further studied.

H. cumingii are shellfish with an open-tube circulatory system, and dsRNA can circulate into various tissues within the mussel after injection through the adductor muscle. D-type cyclin associated CDK4/6 are activated and are important for the progression of the G1 cell cycle phase (Suryadinata et al., 2010). The cyclin D-Cdk4/6 complex phosphorylates Rb1 family proteins, thus resulting in the synthesis of S-phase factors required for cytokinesis (Martinez-Alonso and Malumbres, 2020). *CCND2* and *CDK6* genes were associated with G1-S phase regulation of the cell cycle (Dong et al., 2018). Quantitative results indicated that *Hc-CCND2* gene expression levels were significantly decreased in *H. cumingii* after knockdown of *Hc-CDK6* gene, indicating that there was a close correlation between Hc-CCND2 and Hc-CDK6, consistent with higher organisms (Malumbres et al., 2004). Knockdown of the *Hc-CDK6* gene altered the distribution of cell cycle phases, as detected by flow cytometry: G0 cells increased, and S phase cells decreased, thus indicating cell cycle arrest in G1/S phase. CDK6 is involved in the regulation of G1 phase, and its silencing slows cell cycle progression (Deng et al., 2017). In tumor cells, silencing of CDK6 inhibits proliferation and hinders cycle progression (Whiteway et al., 2013; Zan et al., 2018; Su et al., 2019; Li et al., 2020). This indicates that the correct expression of CDK6 is necessary for normal cell proliferation.

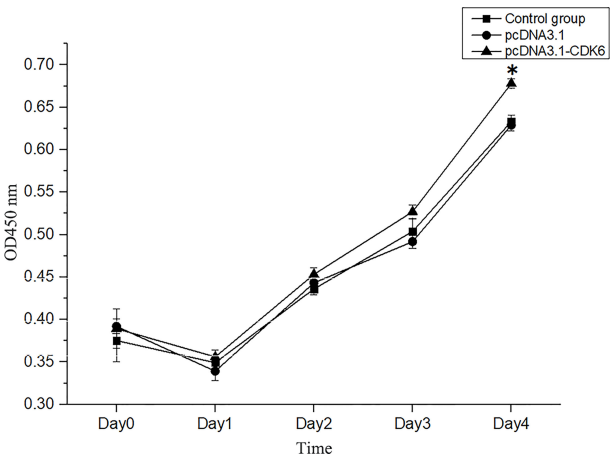

FIGURE 9 | Cell viability assays of transfected and normal *H. cumingii* mantle cells cultured for 0 d, 1 d, 2 d, 3 d and 4 d. *Indicates a significant difference.

The cell cycle is controlled by the synthesis of a single cyclin, and the subsequent activation of CDKs and inactivation of a series of specific Cyclin-CDK complexes at specific cell stages. D-type cyclins and CDK4/6 mainly play roles in the transformation of G1 and promote cell processes. Many studies have shown that overexpression of CCND promoted cell viability and proliferation. In previous studies, increased upstream signal transduction of CCND2 or overexpression of CDK6 has been found to lead to CCND2 accumulation and cell division (Fiaschi-Taesch et al., 2010; Baba et al., 2014). Our previous results showed that highly expressed CCND2 participated in the regulation of the cell cycle and led to the proliferation of mantle cells. Chen et al. have found that the overexpression of CDK6-CCND3 in mouse fibroblasts enhanced their proliferative potential (Chen et al., 2003). CDK6 must be activated with D-type cyclin to function. In this experiment, no difference was observed in cell proliferation activity 3 days after overexpression. D-type cyclin might not have reached the threshold of activating CDK6 activity and thus could not promote cell cycle progression. On the fourth day after transfection, the proliferative activity of

TABLE 2 | Cell proliferation index (Prl) after pcDNA3.1-CDK6 plasmid transfection.

Phase	pcDNA3.1-CDK6 Group	pcDNA3.1 Group	Blank Group
G0/G1 (%)	35.49 ± 0.14^{b}	38.64 ± 0.16^{a}	37.55 ± 0.2^{a}
S (%)	35.77 ± 0.07^{a}	36.47 ± 0.14^{a}	38.60 ± 0.07^{b}
G2 (%)	28.74 ± 0.02^{a}	24.88 ± 0.29^{b}	23.84 ± 0.14^{b}
Prl	0.65 ± 0.02^{a}	0.61 ± 0.01^{b}	0.62 ± 0.01^{b}

Different letters in the same groups represent significant differences (P<0.05).

cells significantly increased, and CCND2 accumulated and reached the threshold for activating CDK6. CDK6 activation promoted cell cycle progression, but the mechanism underlying this regulation by overexpression of CDK6 must be further explored.

In summary, the expression of Hc-CDK6 played an important role in the transformation of G1/S in the cell cycle. After treatment with Hc-CDK6 RNAi, cells were arrested in G0/G1. Overexpression of Hc-CDK6 promoted the proliferation of mantle cells. This study enriched research on the cell cycle in shellfish, providing a basis for further study on cell cycle regulation in shellfish. However, the mechanism of Hc-CDK6 regulated cell cycle has not been identified. Therefore, further study will be necessary for pathway analysis to explore mechanisms of cell cycle regulatory gene interactions.

DATA AVAILABILITY STATEMENT

The datasets presented in this study can be found in online repositories. The names of the repository/repositories and accession number(s) can be found below: https://www.ncbi.nlm.nih.gov/genbank/, OM572509.

ETHICS STATEMENT

The animal study was reviewed and approved by Ethics Committee of Shanghai Ocean University.

AUTHOR CONTRIBUTIONS

SF: performed the experiments and data collection, data analysis and writing; XL: collected the review literature and participated in experimental design; HW: collected the review literature and participated in experiments; WL: performed analysis and experimental design; ZB: revised and submitted the manuscript. All authors contributed to the article and approved the submitted version.

FUNDING

This study was supported by the National Natural Science Foundation of China (31872565), the China Agriculture Research System of MOF and MARA and the Program of Shanghai Academic Research Leader (19XD1421500).

REFERENCES

Baba, Y., Watanabe, M., Murata, A., Shigaki, H., Miyake, K., Ishimoto, T., et al. (2014). LINE-1 Hypomethylation, DNA Copy Number Alterations, and CDK6 Amplification in Esophageal Squamous Cell Carcinoma. *Clin. Cancer Res.* 20, 1114–1124. doi: 10.1158/1078-0432.CCR-13-1645

Cao, Y. X., Lu, A. L., Li, W. J., Shi, Z. Y., and Tao, J. K. (2020). Proliferative Capacity and Biomineralization of Mantle Cells in *Hyriopsis Cumingii* of Different Ages. *J. Fish. Sci. China* 27, 516–523.

Chen, Q., Lin, J., Jinno, S., and Okayama, H. (2003). Overexpression of Cdk6-Cyclin D3 Highly Sensitizes Cells to Physical and Chemical Transformation. *Oncogene* 22, 992–1001. doi: 10.1038/sj.onc.1206193

Deng, M., Zeng, C., Lu, X., He, X., Zhang, R., Qiu, Q., et al. (2017). miR-218 Suppresses Gastric Cancer Cell Cycle Progression Through the CDK6/Cyclin D1/E2F1 Axis in a Feedback Loop. *Cancer Lett.* 403, 175–185. doi: 10.1016/j.canlet.2017.06.006

Dong, P., Zhang, C., Parker, B. T., You, L., and Mathey-Prevot, B. (2018). Cyclin D/CDK4/6 Activity Controls G1 Length in Mammalian Cells. *PloS One* 13, e0185637. doi: 10.1371/journal.pone.0185637

Ericson, K. K., Krull, D., Slomiany, P., and Grossel, M. J. (2003). Expression of Cyclin-Dependent Kinase 6, But Not Cyclin-Dependent Kinase 4, Alters Morphology of Cultured Mouse Astrocytes. *Mol. Cancer Res.* 1, 654–664. doi: 10.1002/mpo.10269

Eyal-Giladi, H., and Kochav, S. (1976). From Cleavage to Primitive Streak Formation: A Complementary Normal Table and a New Look at the First Stages of the Development of the Chick. I. General Morphology. *Dev. Biol.* 49, 321–337. doi: 10.1016/0012-1606(76)90178-0

Fiaschi-Taesch, N. M., Salim, F., Kleinberger, J., Troxell, R., Cozar-Castellano, I., Selk, K., et al. (2010). Induction of Human Beta-Cell Proliferation and Engraftment Using a Single G1/S Regulatory Molecule, Cdk6. *Diabetes* 59, 1926–1936. doi: 10.2337/db09-1776

Fu, X. Y., Shen, Z. H., and Chao, S. L. (1999). Cell Cycle, Restriction Point, Checkpoints. *Chin. Bull. Life Sei.* 11, 31–33.

Guo, J. W., Zhu, X. P., Wu, Z. H., Song, Z. C., Fan, Z. F., Tan, X. G., et al. (2016). Cloning and Expression Analysis of Cdk1 and Cdk6 in Scophthalmus Maximus. *Marine Sci.* 40, 11–21.

Jacobs, T. (1992). Control of the Cell Cycle. *Dev. Biol.* 153, 1–15. doi: 10.1016/0012-1606(92)90087-W

Jin, Y. L., Shi, Z. Y., Li, W. J., Hao, Y. Y., and Qiang, G. (2011). Improvement on Mantle Cell Culture and Technique for Large Nucleated Pearl Producing in *Hyriopsis Cumingii*. *J. Shanghai Ocean Univ.* 20, 705–711.

Kozar, K., and Sicinski, P. (2005). Cell Cycle Progression Without Cyclin D-CDK4 and Cyclin D-CDK6 Complexes. *Cell Cycle* 4, 388–391. doi: 10.4161/cc.4.3.1551

Li, F., Jiang, Z., Shao, X., and Zou, N. (2020). Downregulation of lncRNA NR2F2 Antisense RNA 1 Induces G1 Arrest of Colorectal Cancer Cells by Downregulating Cyclin-Dependent Kinase 6. *Digest. Dis. Sci.* 65, 464–469. doi: 10.1007/s10620-019-05782-5

Lim, S., and Kaldis, P. (2013). Cdks, Cyclins and CKIs: Roles Beyond Cell Cycle Regulation. *Development* 140, 3079–3093. doi: 10.1242/dev.091744

Lin, Y. Q., Geng, J. G., Yang, X. F., and Wang, L. J. (2010). Cell Cycle Control During the Early Stages of Chick Embryo Development. *J. Guangdong Pharm. Univ.* 26, 648–652. doi: 10.3969/j.issn.1006-8783.2010.06.025

Li, Q., Shi, Z. Y., Li, W. J., Huang, K., and Qi, X. X. (2014). Impact of Invitro Optimization and Invivo Implantation Culture on the Growth of *Hyriopsis Cumingii* Mantle Cells. *J. Fish. Sci. China* 21, 225–234. doi: 10.3724/SP.J.1118.2014.00225

Malumbres, M., and Barbacid, M. (2009). Cell Cycle, CDKs and Cancer: A Changing Paradigm. *Nat. Rev. Cancer* 9, 153–166. doi: 10.1038/nrc2602

Malumbres, M., Harlow, E., Hunt, T., Hunter, T., Lahti, J. M., Manning, G., et al. (2009). Cyclin-Dependent Kinases: A Family Portrait. *Nat. Cell Biol.* 11, 1275–1276. doi: 10.1038/ncb1109-1275

Malumbres, M., Sotillo, R., Santamaria, D., Galan, J., Cerezo, A., Ortega, S., et al. (2004). Mammalian Cells Cycle Without the D-Type Cyclin-Dependent Kinases Cdk4 and Cdk6. *Cell* 118, 493–504. doi: 10.1016/j.cell.2004.08.002

Martinez-Alonso, D., and Malumbres, M. (2020). Mammalian Cell Cycle Cyclins. *Semin. Cell Dev. Biol.* 107, 28–35. doi: 10.1016/j.semcdb.2020.03.009

Massague, J. (2004). G1 Cell-Cycle Control and Cancer. *Nature* 432, 298–306. doi: 10.1038/nature03094

Musgrove, E. A., Caldon, C. E., Barraclough, J., Stone, A., and Sutherland, R. L. (2011). Cyclin D as a Therapeutic Target in Cancer. *Nat. Rev. Cancer* 11, 558–572. doi: 10.1038/nrc3090

Pan, B., and Wen, Z. (2002). Farming and Processing of Good Large-Circular Freshwater Pearl. *Modern Fish. Inf.* 17, 15–17. doi: 10.3969/j.issn.1004-8340.2002.02.004

Park, M., and Krause, M. W. (1999). Regulation of Postembryonic G1cell Cycle Progression in Caenorhabditis Elegansby a Cyclin D/CDK-Like Complex. *Development* 126, 4849–4860. doi: 10.1242/dev.126.21.4849

Pietenpol, J. A., and Stewart, Z. A. (2002). Cell Cycle Checkpoint Signaling: Cell Cycle Arrest Versus Apoptosis. *Toxicology*, 181–182, 475–481. doi: 10.1016/S0300-483X(02)00460-2

Pines, J., and Hunter, T. (1991). Cyclin-Dependent Kinases: A New Cell Cycle Motif? *Trends Cell Biol.* 1, 117–121. doi: 10.1016/0962-8924(91)90116-Q

Qian, W. P., Xu, Z. R., Zhang, M. X., and Shi, M. Q. (2002). Study on Culturing Pearl Sacs *In Vitro* and Injection Method for Pearl Producing. *Acta Agricult. Zhejiangensis* 14, 82–86. doi: 10.3969/j.issn.1004-1524.2002.02.004

Satyanarayana, A., and Kaldis, P. (2009). Mammalian Cell-Cycle Regulation: Several Cdks, Numerous Cyclins and Diverse Compensatory Mechanisms. *Oncogene* 28, 2925–2939. doi: 10.1038/onc.2009.170

Schaer, D. A., Beckmann, R. P., Dempsey, J. A., Huber, L., Forest, A., Amaladas, N., et al. (2018). The CDK4/6 Inhibitor Abemaciclib Induces a T Cell Inflamed Tumor Microenvironment and Enhances the Efficacy of PD-L1 Checkpoint Blockade. *Cell Rep.* 22, 2978–2994. doi: 10.1016/j.celrep.2018.02.053

Su, H., Chang, J., Xu, M., Sun, R., and Wang, J. (2019). CDK6 Overexpression Resulted From Microrna320d Downregulation Promotes Cell Proliferation in Diffuse Large Bcell Lymphoma. *Oncol. Rep.* 42, 321–327. doi: 10.3892/or.2019.7144

Suryadinata, R., Sadowski, M., and Sarcevic, B. (2010). Control of Cell Cycle Progression by Phosphorylation of Cyclin-Dependent Kinase (CDK) Substrates. *Biosci. Rep.* 30, 243–255. doi: 10.1042/BSR20090171

Tigan, A. S., Bellutti, F., Kollmann, K., Tebb, G., and Sexl, V. (2016). CDK6-A Review of the Past and a Glimpse Into the Future: From Cell-Cycle Control to Transcriptional Regulation. *Oncogene* 35, 3083–3091. doi: 10.1038/onc.2015.407

Wang, Y., Chen, Y., Cao, M., Wang, X., Wang, G., and Li, J. (2021a). Identification of Wnt2 in the Pearl Mussel Hyriopsis Cumingii and its Role in Innate Immunity and Gonadal Development. *Fish Shellfish Immunol.* 118, 85–93. doi: 10.1016/j.fsi.2021.08.022

Wang, Y., Wang, X., Ge, J., Wang, G., and Li, J. (2021b). Identification and Functional Analysis of the Sex-Determiner Transformer-2 Homologue in the Freshwater Pearl Mussel, Hyriopsis Cumingii. *Front. Physiol.* 12, 704548. doi: 10.3389/fphys.2021.704548

Whiteway, S. L., Harris, P. S., Venkataraman, S., Alimova, I., Birks, D. K., Donson, A. M., et al. (2013). Inhibition of Cyclin-Dependent Kinase 6 Suppresses Cell Proliferation and Enhances Radiation Sensitivity in Medulloblastoma Cells. *J. Neuro Oncol.* 111, 113–121. doi: 10.1007/s11060-012-1000-7

Zan, P. F., Yao, J., Wu, Z., Yang, Y., Hu, S., and Li, G. D. (2018). Cyclin D1 Gene Silencing Promotes IL-1beta-Induced Apoptosis in Rat Chondrocytes. *J. Cell. Biochem.* 119, 290–299. doi: 10.1002/jcb.26172

Conflict of Interest: The authors declare that the research was conducted in the absence of any commercial or financial relationships that could be construed as a potential conflict of interest.

Publisher's Note: All claims expressed in this article are solely those of the authors and do not necessarily represent those of their affiliated organizations, or those of the publisher, the editors and the reviewers. Any product that may be evaluated in this article, or claim that may be made by its manufacturer, is not guaranteed or endorsed by the publisher.